Journal of Chromatography B, 877 (2009) 2639–2647

Contents lists available at ScienceDirect

Journal of Chromatography B

journal homepage: www.elsevier.com/locate/chromb

Global analysis of triacylglycerols including oxidized molecular species by reverse-phase high resolution LC/ESI-QTOF MS/MS☆

Kazutaka Ikeda[a,b], Yuichi Oike[c], Takao Shimizu[d], Ryo Taguchi[a,b,*]

[a] Department of Metabolome, Graduate School of Medicine, The University of Tokyo, Bunkyo-ku, Tokyo 113-0033, Japan
[b] CREST, Japan Science and Technology Agency (JST), Kawaguchi, Saitama 332-0012, Japan
[c] Department of Molecular Genetics, Graduate School of Medical Sciences, Kumamoto University, Kumamoto 860-0811, Japan
[d] Department of Biochemistry and Molecular Biology, Faculty of Medicine, The University of Tokyo, Bunkyo-ku, Tokyo 113-0033, Japan

ARTICLE INFO

Article history:
Received 1 October 2008
Accepted 31 March 2009
Available online 7 April 2009

Keywords:
Triacylglycerol
Global analysis
Two-dimensional profiling
Lipidomics

ABSTRACT

Recently, global analysis of triacylglycerols (TAGs) has become increasingly important in studies of abnormality of lipid metabolism in metabolic syndrome. TAGs consist of various molecular species, caused by their three fatty acyl chains with a large variety of carbon chain lengths and degrees of unsaturation. Therefore, most previously reported methods have been insufficient in global detection of TAGs including their structural isomers and TAGs with oxidized or odd number acyl carbon chain. Here we report an effective method for global analysis of TAG molecular species from complex lipid mixtures of mouse liver and white adipose tissue (WAT) using reverse-phased high resolution liquid chromatography (LC) coupled with electrospray ionization (ESI)-quadrapole/time of flight hybrid mass spectrometer (QTOF-MS). For effective profiling of TAG molecular species, sensitive two-dimensional (2D) maps were constructed and individual structures were correctly identified by the elution profile and MS/MS. As a result, TAGs including their structural isomers and TAGs with an odd number acyl carbon chain were separated and detected effectively on the 2D map as compared with conventional high performance LC. It was also found that our 2D profiling method was useful in searching characteristic molecular species globally. In mouse WAT, novel oxidized TAGs, which were mainly formed by hydroperoxidation of one of their linoleic acyl chains, were effectively detected in comparison with TAG molecular species of mouse liver.

1. Introduction

Excessive accumulation of triacylglycerols (TAGs) in liver and adipose tissue is one of the risk factors for the metabolic syndrome [1,2]. Therefore, global analysis of TAGs becomes important to elucidate the pathology. The current analytical methods for TAGs include clinical colorimetric kits using lipoprotein lipase (LPL) to hydrolyze the fatty acids from the TAGs [3–5]. However, determination of the specific TAG molecular species is difficult using these kits, because they nonspecifically analyze the fatty acids released by LPL. Thus, an alternative approach that utilizes liquid chromatography (LC) coupled with electrospray ionization mass spectrometry (ESI-MS) and atmospheric pressure chemical ionization mass spectrometry (APCI-MS) has received interest for detailed structural analysis of TAGs [6–8]. In particular, LC/ESI-MS is considered to be a useful soft ionization method and effective in quantification and identification of TAG molecular species [9–13]. A recent application of ESI-MS for TAG analysis has involved neutral loss scanning of the fatty acyl chains and this method has been used frequently and effectively in distinguishing TAG molecular species from complex lipid mixtures extracted by Bligh and Dyer's method [14–16]. But, neutral loss scanning is insufficient to discriminate among the close m/z value TAGs such as normal TAGs and modified TAGs with oxidized acyl carbon chain and to permit quantitative determination of the structural isomers without separating them by LC. For these reasons, this scanning is difficult to detect a variety of TAGs globally and quantitatively.

Therefore, we attempted to establish an effective method for global analysis of TAG molecular species in complex lipid mixtures of mouse liver and white adipose tissue (WAT) using reverse-phased ultra-performance liquid chromatography (UPLC) coupled with ESI-MS using a quadrapole/time of flight hybrid mass spectrometer (QTOF-MS) with high mass accuracy. The high resolution LC allows an increase in separation efficiency due to the reduced particle size and fits for analysis of TAGs including many complex molecular species such as structural isomers.

☆ This paper was presented at the 33rd Meeting of the Japanese Society for Biomedical Mass Spectrometry, Tokyo, Japan, 25–26 September 2008.

* Corresponding author at: Department of Metabolome, Graduate School of Medicine, The University of Tokyo, Bunkyo-ku, Tokyo 113-0033, Japan.
Tel.: +81 3 5841 3650; fax: +81 3 5841 3430.
E-mail address: rytagu@m.u-tokyo.ac.jp (R. Taguchi).

1570-0232/$ – see front matter © 2009 Elsevier B.V. All rights reserved.
doi:10.1016/j.jchromb.2009.03.047

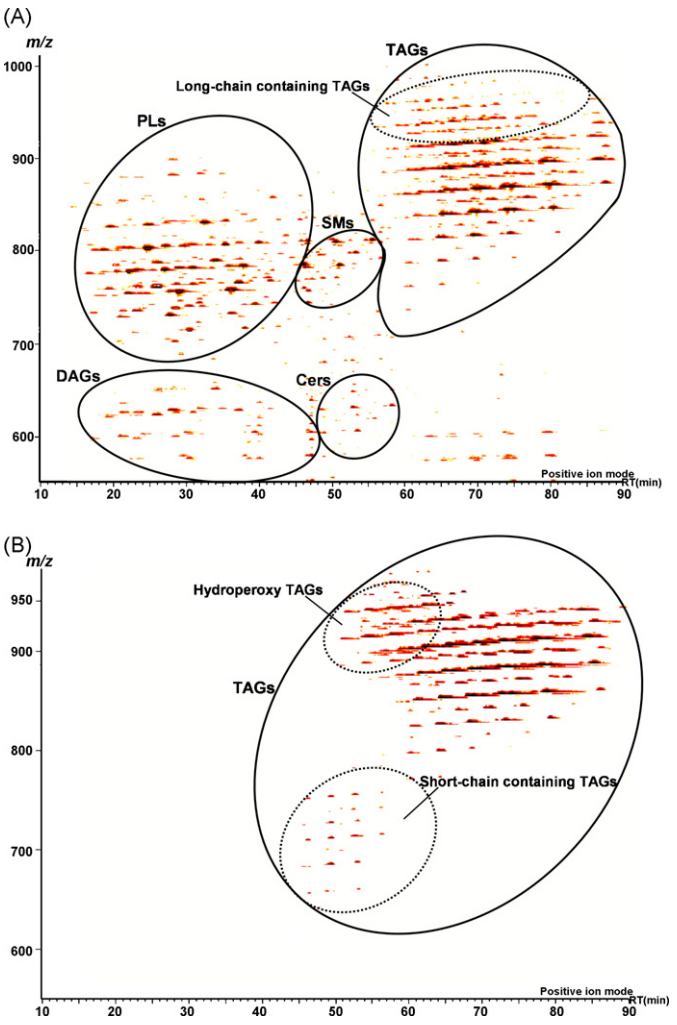

Fig. 1. Two-dimensional (2D) maps of complex lipid mixtures from mouse liver and white adipose tissue (WAT) by reverse-phase high resolution LC/ESI-QTOF MS analysis. The lipid mixtures of mouse liver were eluted in the following order: PLs = DAGs > SMs = Cers > TAGs (panel A). TAGs containing long fatty acyl chains were characteristically detected in mouse liver. Meanwhile, the lipid mixtures of WAT were mainly constituted of TAGs, and hydroperoxy TAGs and TAGs containing short fatty acyl chain were distinctively found among them (panel B). The 2D maps was constructed with *X* (retention time) and *Y* (*m*/*z* value) axes, and abundance of individual TAGs was indicated by single color density (originally adjusted by color gradient).

We also created two-dimensional (2D) profiling maps of individual precursor ions of TAGs, constructed with *X* (retention time) and *Y* (*m*/*z* value) axes, and abundance of the individual TAGs was adjusted by the color density [9,10]. For detailed profiling of the TAG molecular species of mouse liver and WAT, these TAG structures were analyzed by the elution profile and MS/MS, and these profiling maps were compared for investigation of the distinctive TAG distributions.

2. Experimental

2.1. Materials

Acetic acid, acetonitrile, chloroform, isopropanol and methanol with LC grade, 28% aqueous ammonia were purchased from Wako Pure Chemicals (Osaka, Japan).

Deionized water was obtained using a Milli-Q water system (Millipore, Milford, MA, USA).

2.2. Preparation of samples

TAGs in C57BL/6 mouse (purchased from SLC, Shizuoka, Japan) liver (100 mg) and WAT (100 mg) were extracted using Bligh and Dyer's method in the following procedure [16]: the liver and WAT were homogenized with 6 mL chloroform/methanol (1:2) for 10 strokes and left for 1 h at room temperature. Each phase separation was achieved by adding 2 mL chloroform and 2 mL water. After vortexing, the mixture was centrifuged at 3000 rpm for 10 min. The bottom organic layer containing the total lipid extract was collected and dried under a gentle stream of nitrogen, and then dissolved in chloroform/methanol (2:1) at a concentration of 10 μg (tissue weight)/μL.

2.3. LC conditions

Reverse-phased LC separation was achieved using ACQUITY UPLC BEH column (1.0 mm × 150 mm i.d., particle size 1.7 μm, Waters Corporation, Milford, MA, USA) at 45 °C. The mobile phase was acetonitrile/methanol/water: 19/19/2 (0.1% acetic acid + 0.028% ammonia) (A), and isopropanol (0.1% acetic acid + 0.028% ammonia) (B), and the composition was produced by mixing these solvents. The gradient consisted of holding solvent (A/B:90/10) for 5 min, then linearly converting to solvent (A/B:60/40) for 35 min and then linearly converting solvent (A/B:45/55) for 50 min. The mobile phase was pumped at a flow rate of 50 μL/min and the column pressure was adjusted lower than 5000 psi. Typically, 2 μL of sample solution was injected.

2.4. ESI-MS conditions

The ESI-MS analysis was performed using a quadrapole/time of flight hybrid mass spectrometer (QTOF micro™, Micromass, Manchester, UK) with an ACQUITY UPLC system (Waters Corporation). The mass range of the instrument was set at *m*/*z* 200–1100 and scan duration of MS and MS/MS at 0.5 s in positive ion mode. The capillary voltage was set at 3.5 kV, cone voltage at 30 V, and source block temperature at 100 °C. The collision gas used for MS/MS experiments was argon (7.5×10^5 mbar), and the collision energy was set at 30 V.2D map of individual precursor ions of TAGs, constructed with *X* (retention time) and *Y* (*m*/*z* value) axes, and abundance of individual TAGs was indicated by single color density in figures (originally adjusted by color gradient).

3. Results and discussion

3.1. 2D profiling analysis of TG molecular species from mouse liver and WAT

Individual lipid molecules of complex lipid mixtures from mouse liver and WAT were easily assigned for 90 min as shown by these 2D maps (*X*-axis: retention time; *Y*-axis: *m*/*z* value) (Fig. 1A and B); the lipid molecules were eluted in the following order: phospholipids (PLs) = diacylglycerols (DAGs) > sphingomyelins (SMs) = ceramides (Cers) > TAGs. Even without purification of these TAGs from the complex lipid mixtures, individual TAG molecular species were separated and the distribution differences between mouse liver and WAT were visually obtainable in our method. In mouse liver, TAGs containing long fatty acyl chains, whose total carbon chain length were more than 58, were characteristically detected (panel A). Even though PLs, DAGs, SMs and Cers were also contained in mouse liver, TAGs were mainly included in mouse WAT. In addition, hydroperoxy TAGs and TAGs containing short fatty acyl chain, whose total carbon chain length were less than 42, were distinctively found among them (panel B).

Table 1
Major TAG molecular species from mouse liver identified by MS/MS analysis.

Total chain length (C_N)	Total degree of unsaturation (U_N)	m/z ([M+NH_4]$^+$)	Identified TAG molecular species	Retention time (min)
64	14	1020.80	18:2–22:6–24:6	61.8
	13	1022.82	18:2–22:6–24:5	64.5
	12	1024.83	18:1–22:6–24:5	68.4
62	14	992.77	18:2–22:6–22:6	59.1
	13	994.79	18:2–22:5–22:6/18:1–22:6–22:6	60.8/63.0
	12	996.80	18:1–22:5–22:6	64.6
	11	998.82	18:0–22:5–22:6	68.6
60	13	966.76	18:2–20:5–22:6	57.6
	12	968.77	18:2–20:4–22:6/16:0–22:6–22:6	61.2/63.2
	11	970.79	18:1–20:4–22:6	64.8
	10	972.80	18:2–18:2–24:6	67.1
	9	974.82	18:1–18:2–24:6/18:2–20:1–22:6	69.1/70.7
	8	976.83	18:1–18:1–24:6/18:1–20:1–22:6	72.0/73.2
58	12	940.74	16:1–20:5–22:6	56.3
	11	942.76	16:1–20:4–22:6	59.3
	10	944.77	18:2–18:2–22:6/16:0–20:4:22:6	62.6/65.2
	9	946.79	18:2–18:2–22:5/18:1–18:2–22:6	64.4/66.5
	8	948.80	16:0–18:2–24:6/18:1–18:2–22:5	68.2/70.5
	7	950.82	18:0–18:2–22:5/18:0–18:1–22:6	72.1/75.4
	6	952.83	16:0–18:1–24:5	76.4
56	10	916.74	18:2–18:3–20:5/16:1–18:3–22:6	57.7/58.6
	9	918.76	18:2–18:2–20:5/16:1–18:2–22:6	61.1/62.2
	8	920.77	16:1–18:2–22:5	66.8
	7	922.79	16:0–18:2–22:5/16:0–18:1–22:6	68.6/70.8
	6	924.80	16:0–18:1–22:5	72.5
	5	926.82	16:0–18:0–22:5/16:0–18:1–22:4/18:0–18:1–20:4	75.2/76.6/78.3
	4	928.83	18:1–18:2–20:1	79.6
	3	930.85	18:1–18:1–20:1	85.6
54	8	892.74	18:2–18:3–18:3	60.7
	7	894.76	18:2–18:2–18:3/16:0–18:2–20:5	62.7/65.4
	6	896.77	18:2–18:2–18:2/18:1–18:2–18:3/16:0–18:2–20:4	66.4/67.5/68.7
	5	898.79	18:1–18:2–18:2/18:0–18:2–18:3/16:0–18:1–20:4	70.3/71.2/72.8
	4	900.80	18:1–18:1–18:2/18:0–18:2–18:2	74.1/75.4
	3	902.82	18:1–18:1–18:1/18:0–18:1–18:2	79.3/80.5
	2	904.83	18:0–18:1–18:1	86.7
53	5	884.77	17:1–18:2–18:2	68.0
	4	886.79	17:0–18:2–18:2	72.0
	3	888.80	17:0–18:1–18:2/17:1–18:1–18:1	76.5/77.3
	2	890.82	17:0–18:1–18:1	83.2
52	6	868.74	16:1–18:2–18:3/16:0–16:1–20:5	62.1/64.1
	5	870.76	16:1–18:2–18:2/16:0–18:2–18:3	66.0/67.1
	4	872.77	16:1–18:1–18:2/16:0–18:2–18:2	69.8/70.8
	3	874.79	16:1–18:1–18:1/16:0–18:1–18:2	73.7/74.9
	2	876.80	16:0–18:1–18:1/16:0–18:0–18:2	79.8/81.0
	1	878.82	16:0–18:0–18:1	67.8
51	4	858.76	15:0–18:2–18:2	68.2
	3	860.77	15:0–18:1–18:2	72.3
	2	862.82	15:0–18:1–18:1	77.0
	1	864.80	15:0–18:0–18:1	84.0
50	5	842.72	16:1–16:1–18:3/14:0–18:2–18:3	61.7/62.4
	4	844.74	16:1–16:1–18:2/14:0–18:2–18:2/16:0–16:1–18:3	65.2/65.8/66.4
	3	846.76	16:1–16:1–18:1/16:0–16:1–18:2/16:0–16:0–18:3	69.1/70.1/71.1
	2	848.77	16:0–16:1–18:1/16:0–16:0–18:2	74.1/75.2
	1	850.79	16:0–16:0–18:1	80.5
49	3	832.74	15:0–16:1–18:2	67.7
	2	834.76	15:0–16:0–18:2	72.1
	1	836.77	15:0–16:0–18:1	77.3
48	4	816.71	12:0–18:2–18:2/14:0–16:1–18:3	61.1/61.7
	3	818.72	14:0–16:1–18:2/14:0–16:0–18:3	65.5/66.4
	2	820.74	14:0–16:1–18:1/14:0–16:0–18:2	69.3/70.2
	1	822.76	14:0–16:0–18:1	74.4
	0	824.77	16:0–16:0–16:0	81.2
46	2	792.71	12:0–16:1–18:1/12:0–16:0–18:2	64.9/65.6
	1	794.72	12:0–16:0–18:1	69.7
	0	796.74	14:0–16:0–16:0	75.2
44	2	764.68	10:0–16:0–18:2	60.8
	1	766.69	10:0–16:0–18:1	65.2

Individual structures of these TAG molecular species were confirmed by the MS/MS analysis.

Table 2
Major TAG molecular species from mouse WAT identified by MS/MS analysis.

Total chain length (C_N)	Total degree of unsaturation (U_N)	m/z ($[M+NH_4]^+$)	Identified hydroperoxy TAG molecular species	Retention time (min)
54	6	928.76	18:2–18:2–18:2[OOH]	50.6
	5	930.78	18:1–18:2–18:2[OOH]	54.0
	4	932.79	18:1–18:1–18:2[OOH]	56.8
	3	934.81	18:0–18:1–18:2[OOH]	61.1
52	5	902.74	16:1–18:2–18:2[OOH]	50.5
	4	904.76	16:0–18:2–18:2[OOH]	53.3
	3	906.78	16:0–18:1–18:2[OOH]	56.6
50	4	876.73	16:1–16:1–18:2[OOH]	50.1
	3	878.74	16:0–16:1–18:2[OOH]	53.2
	2	880.76	16:0–16:0–18:2[OOH]	56.9

Total chain length (C_N)	Total degree of unsaturation (U_N)	m/z ($[M+NH_4]^+$)	Identified TAG molecular species	Retention time (min)
56	9	918.76	18:2–18:2–20:5/16:1–18:2–22:6	59.7/60.6
	8	920.77	18:2–18:2–20:4/18:1–18:2–20:5	61.9/63.0
	7	922.79	16:0–18:2–22:5	66.2
	6	924.80	18:1–18:1–20:4/16:0–18:1–22:5	68.7/69.7
54	7	894.76	18:2–18:2–18:3/16:1–18:1–20:5/16:0–18:2–20:5	61.0/62.8/63.3
	6	896.77	18:2–18:2–18:2/18:1–18:2–18:3	64.3/66.1
	5	898.79	18:1–18:2–18:2	67.2
	4	900.80	18:1–18:1–18:2/18:0–18:2–18:2	71.0/72.5
	3	902.82	18:1–18:1–18:1/18:0–18:1–18:2	75.1/76.6
	2	904.83	18:0–18:1–18:1	81.5
53	5	884.77	17:1–18:2–18:2	65.7
	4	886.79	17:1–18:1–18:2/17:0–18:2–18:2	69.1/69.9
	3	888.80	17:1–18:1–18:1/17:0–18:1–18:2	72.8/73.7
	2	890.82	17:0–18:1–18:1	78.5
52	6	868.74	16:1–18:2–18:3/16:0–18:3–18:3	60.5/61.7
	5	870.76	16:1–18:2–18:2/16:0–18:2–18:3	63.5/64.5
	4	872.77	16:1–18:1–18:2/16:0–18:2–18:2	67.1/68.4
	3	874.79	16:1–18:1–18:1/16:0–18:1–18:2	70.7/71.9
	2	876.80	16:0–18:1–18:1/16:0–18:0–18:2	75.8/77.1
	1	878.82	16:0–18:0–18:1	82.5
51	3	860.77	15:0–18:1–18:2	69.6
	2	862.82	15:0–18:1–18:1/16:0–17:1–18:1	73.2/74.2
	1	864.80	16:0–17:0–18:1	79.1
50	5	842.72	16:1–16:1–18:3/14:0–18:2–18:3	60.0/60.8
	4	844.74	16:1–16:1–18:2/14:0–18:2–18:2/16:0–16:1–18:3	63.0/63.6/64.5
	3	846.76	16:1–16:1–18:1/16:0–16:1–18:2/16:0–16:0–18:3	66.6/67.3/68.7
	2	848.77	16:0–16:1–18:1/16:0–16:0–18:2	71.1/72.2
	1	850.79	16:0–16:0–18:1	76.6
	0	852.80	16:0–16:0–18:0	83.3
49	3	832.74	15:0–16:1–18:2	65.5
	2	834.76	15:0–16:0–18:2	69.9
	1	836.77	15:0–16:0–18:1	73.7
48	4	816.71	12:0–18:2–18:2/14:0–16:1–18:3	59.4/60.3
	3	818.72	14:0–16:1–18:2/14:0–16:0–18:3	63.1/64.5
	2	820.74	14:0–16:1–18:1/14:0–16:0–18:2	66.9/67.8
	1	822.76	14:0–16:0–18:1	71.6
	0	824.77	16:0–16:0–16:0	72.2
47	2	806.72	13:0–16:0–18:2	65.6
	1	808.74	13:0–16:0–18:1	70.0
	0	810.76	13:0–16:0–18:0	74.1
46	4	788.68	10:0–18:2–18:2	55.6
	3	790.69	10:0–18:1–18:2/12:0–16:0–18:3	59.2/60.2
	2	792.71	12:0–16:1–18:1/12:0–16:0–18:2	62.8/63.5
	1	794.72	12:0–16:0–18:1	67.2
	0	796.74	14:0–16:0–16:0	72.2
44	3	762.66	10:0–16:1–18:2	55.2
	2	764.68	10:0–16:0–18:2	59.1
	1	766.69	10:0–16:0–18:1	63.0
	0	768.71	12:0–16:0–16:0	67.5
42	3	734.63	6:0–18:1–18:2	51.6
	2	736.65	12:0–12:0–18:2	55.0
	1	738.66	12:0–12:0–18:1	58.7
	0	740.68	12:0–14:0–16:0	63.2
40	3	706.60	4:0–18:1–18:2	48.5
	2	708.61	6:0–16:0–18:2	51.8

Table 2 (*Continued*)

Total chain length (C_N)	Total degree of unsaturation (U_N)	m/z ($[M+NH_4]^+$)	Identified TAG molecular species	Retention time (min)
	1	710.63	6:0–16:0–18:1	55.3
	0	712.65	12:0–14:0–14:0	59.0
38	2	680.58	4:0–16:0–18:2	48.6
	1	682.60	4:0–16:0–18:1	52.1

Individual structures of these TAG molecular species were confirmed by the MS/MS analysis.

3.2. MS/MS analysis of major TAGs from mouse liver and WAT

For detailed analysis of these TAG structures, each spot on the 2D maps was analyzed by MS/MS. In the MS/MS analysis, DAG ion products ($[DAG-OH]^+$) were produced by loss of the fatty acyl residue from the TAG ion ($[M+NH_4]^+$), and the constitution of the individual fatty acyl chains was revealed by calculation of the lost fatty acyl residue [6,7,17]. Monoacylglycerol (MAG) ion products ($[MAG-OH]^+$) were derived from loss of the two fatty acyl residues, and structure of the individual fatty acyl chains was directly understandable. For example, MS/MS fragmentation of TAG ion ($[M+NH_4]^+$; m/z 918.76 from mouse

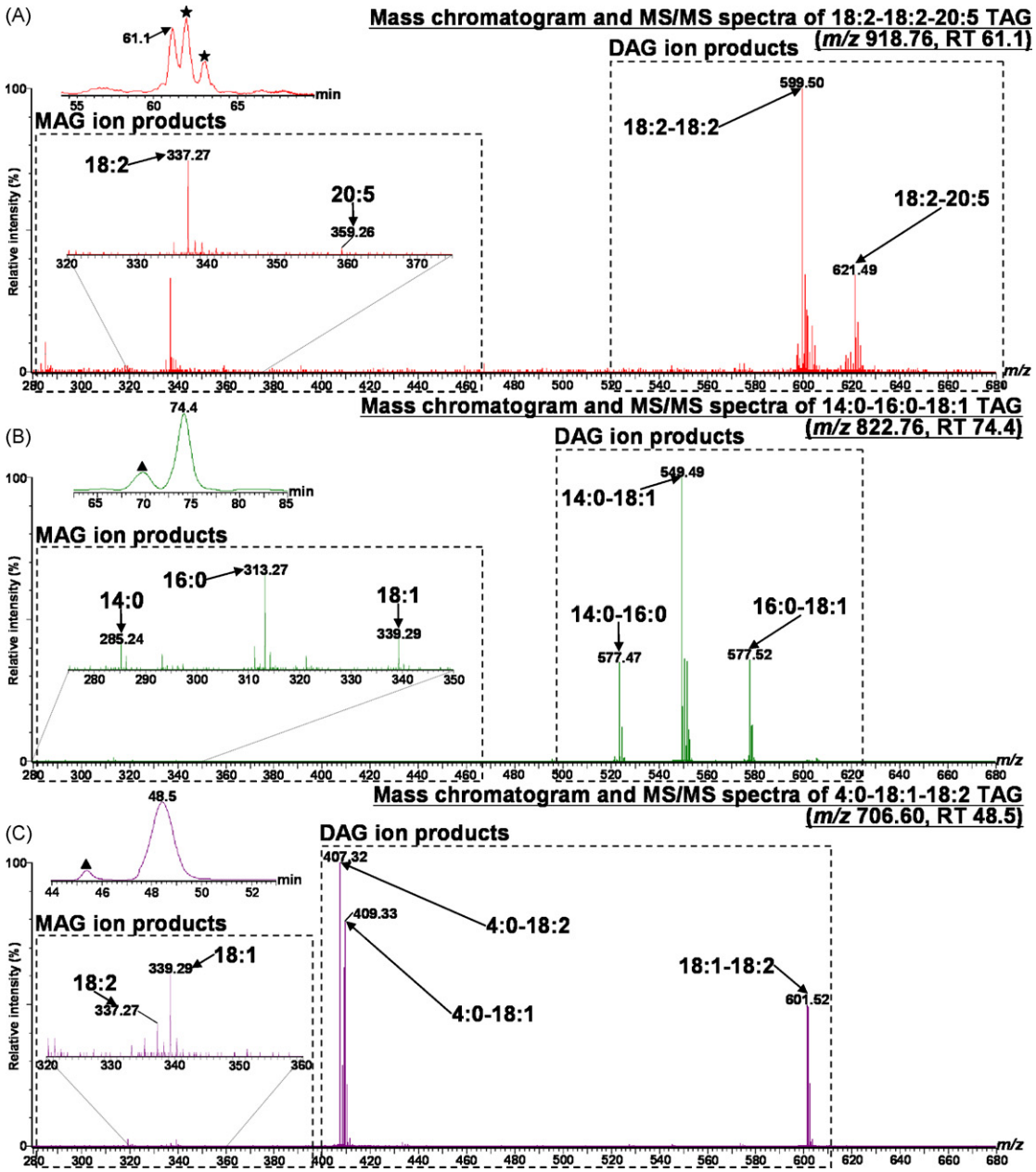

Fig. 2. Mass chromatogram and MS/MS spectra of (A) 18:2–18:2–20:5 (m/z 918.76), (B) 14:0–16:0–18:1 (m/z 822.76) and (C) 4:0–18:1–18:2 (m/z 706.60) TAGs by reverse-phase high resolution LC/ESI-QTOF MS/MS analysis. Each TAG structure was determined based on individual DAG ion products ($[DAG-OH]^+$ produced by loss of the fatty acyl residue from the TAG ion) and MAG ion products ($[MAG-OH]^+$ produced by loss of the two fatty acyl residues from the TAG ion). The structural isomeric and isotopic peaks of other molecular species, and retention time were respectively indicated by starburst (⋆), triangle (▲) and RT.

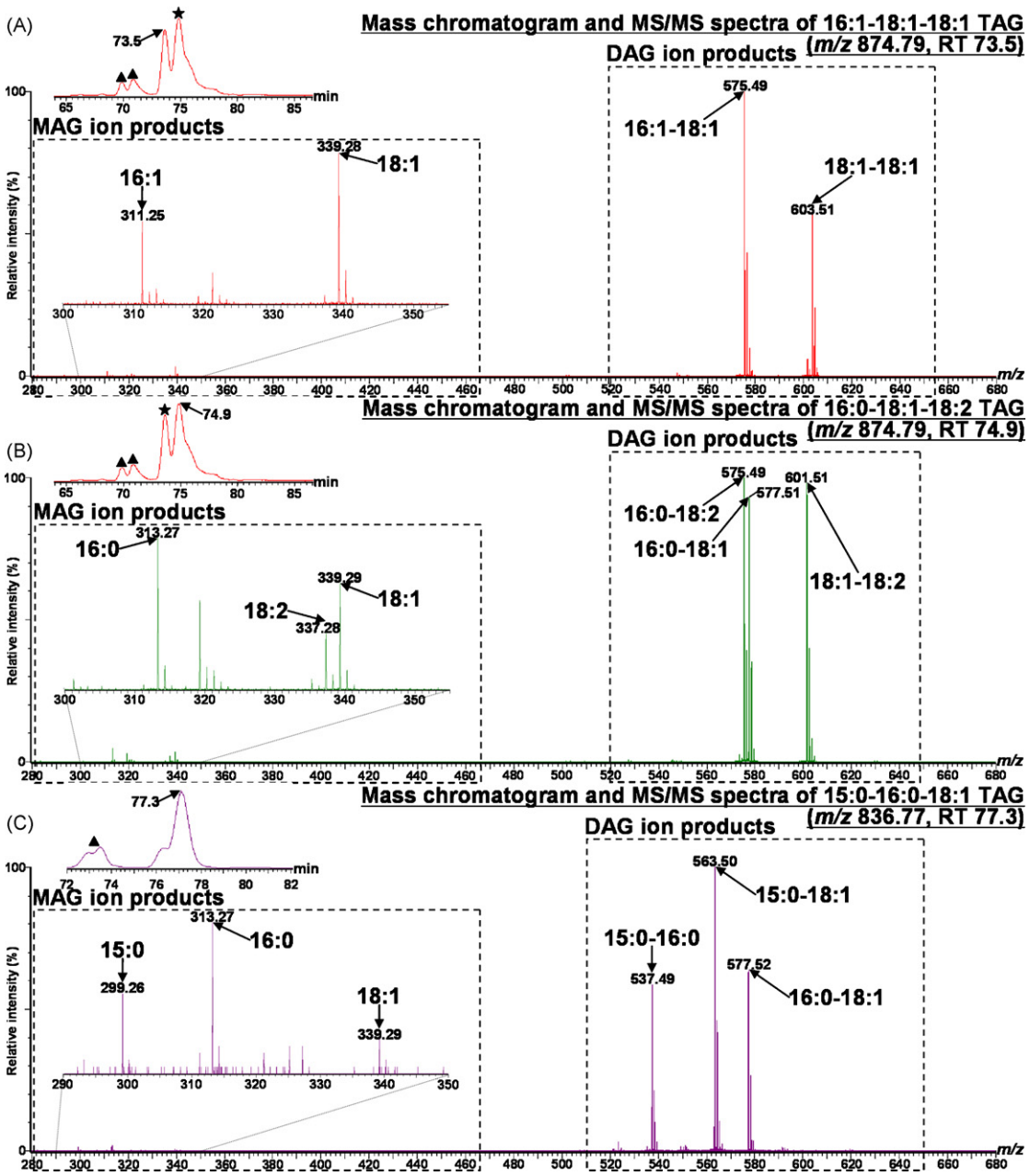

Fig. 3. Mass chromatogram and MS/MS spectra of (A) 16:1–18:1–18:1 and (B) 16:0–18:1–18:2 (*m*/*z* 874.79) TAG structural isomers, and (C) 15:0–16:0–18:1 (*m*/*z* 836.77) TAG with an odd number acyl carbon chain by reverse-phase high resolution LC/ESI-QTOF MS/MS analysis. Each TAG structural isomer and TAG with an odd number acyl carbon chain were successfully separated and identified by the individual DAG ion products ($[DAG-OH]^+$) and MAG ion products ($[MAG-OH]^+$). The structural isomeric and isotopic peaks of other molecular species were respectively indicated by starburst (⋆) and triangle (▲).

liver) produced DAG ion products (*m*/*z* 621.49 → 18:2–20:5, *m*/*z* 599.50 → 18:2–18:2) and MAG ion products (*m*/*z* 359.26 → 20:5, *m*/*z* 337.27 → 18:2) (Fig. 2A). From these MS/MS spectra, it was identified as 18:2–18:2–20:5 TAG containing long-chain polyunsaturated fatty acids (PUFAs). Similarly, 14:0–16:0–18:1 TAG (*m*/*z* 822.76 from mouse liver) containing saturated fatty acid (SFA) and monounsaturated fatty acid (MUFA) and 4:0–18:1–18:2 TAG (*m*/*z* 706.60 from mouse WAT) containing a short-chain fatty acid were determined based on individual DAG and MAG ion products (Fig. 2B and C).

Our method also allowed us to separate and distinguish TAG structural isomers. For example, each of the structural isomers (*m*/*z* 874.79 from mouse liver), which was difficult to separate by our conventional reverse-phased LC (data not shown), was successfully separated and respectively identified as 16:1–18:1–18:1 (A) and 16:0–18:1–18:2 (B) based on individual DAG and MAG ion products (Fig. 3A and B).

Furthermore, some spots were detected other than these major TAGs on the 2D maps. As a result of MS/MS analysis, they were found to be TAGs containing an odd number acyl carbon chain. For example, MS/MS fragmentation of TAG ion ($[M+NH_4]^+$; *m*/*z* 836.77 from mouse liver) produced DAG ion products ($[DAG-OH]^+$; *m*/*z* 577.52 → 16:0–18:1, *m*/*z* 563.50 → 15:0–18:1, *m*/*z* 537.49 → 15:0–16:0) and MAG ion products ($[MAG-OH]^+$; *m*/*z* 339.29 → 18:1, *m*/*z* 313.27 → 16:0, *m*/*z* 299.26 → 15:0) (Fig. 3C). From these MS/MS spectra, it was identified as 15:0–16:0–18:1 TAG. Our method enabled us to detect globally not only major TAGs including these structural isomers but also TAGs with an odd number acyl carbon chain (Tables 1 and 2).

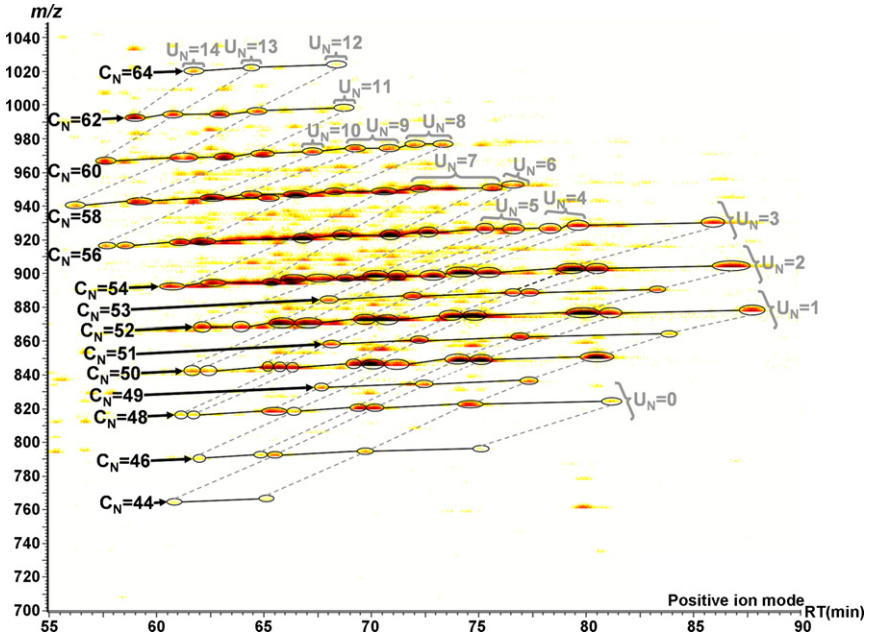

Fig. 4. 2D map of TAG molecular species from mouse liver by reverse-phase high resolution LC/ESI-QTOF MS/MS analysis. Individual TAG molecular species identified by the MS/MS analysis were present on the 2D map. Many of TAGs containing long-chain polyunsaturated fatty acids (PUFAs) were characteristically detected in mouse liver. TAGs with the same total carbon chain length (C_N) and TAGs with the same total degree of unsaturation (U_N) were respectively indicated by solid line and dotted line. Some spots on the 2D map were not unidentified by MS/MS analysis, but most of them were readily predicted by the elution regularity.

From the presentation of individual TAG structures on the 2D map of mouse liver, it revealed that TAGs containing short-chain SFA and MUFA, and TAGs containing long-chain PUFAs were eluted relatively earlier than other TAGs as previously reported with PLs (Fig. 4) [9,10]. Furthermore, TAGs containing a higher degree of unsaturated fatty acid were eluted earlier among the TAGs with the same total carbon chain length. In addition, TAGs containing shorter chain lengths were eluted earlier among the TAGs with the same degree of unsaturation. These results show that TAG molecular species are regularly eluted according to their carbon chain lengths and degrees of unsaturation, and individual TAG structures, despite minor TAG molecular species, are readily predicted by the elution regularity from the 2D map, even if MS/MS analysis are difficult for the small amount.

3.3. Detection of novel hydroperoxy TAGs from mouse WAT

WAT is thought to serve as the primary energy depot in the body by storing TAGs and investigation of the distinctive TAG distributions might be important in elucidating obesity. We then performed profiling analysis of TAG molecular species by applying our method to mouse WAT.

Compared with TAG profiling of mouse liver (Fig. 1A), a number of TAGs eluted earlier were detected on the 2D map (Fig. 1B).

For elucidation of these TAG structures, they were analyzed by MS/MS. For example, MS/MS fragmentation of TAG ion ($[M+NH_4]^+$; m/z 932.79) produced hydroperoxy DAG ion products (produced by loss of H_2O or H_2O_2 from $[\text{hydroperoxy DAG}-OH]^+$ derived from loss of the fatty acyl residue from the TAG ion; m/z 615.50 → [18:1–18:2(OOH)]–H_2O, m/z 599.50 → [18:1–18:2(OOH)]–H_2O_2) and DAG ion product ($[DAG-OH]^+$ produced by loss of the hydroperoxy linoleic acyl chain from the TAG ion; m/z 603.54 → 18:1–18:1), and hydroperoxy MAG ion products (produced by loss of H_2O or $2H_2O$ from $[\text{hydroperoxy MAG}-OH]^+$ derived from loss of the two fatty acyl residues from the TAG ion; m/z 351.25 → [18:2(OOH)]–H_2O, m/z 333.24 → [18:2(OOH)]–$2H_2O$) and MAG ion product ($[18:1\text{-}OH]^+$; m/z 339.29 produced by loss of the hydroperoxy acyl chain and fatty acyl residue from the TAG ion) (Fig. 5A) [18]. Thus, this TAG was composed of 18:1–18:1–18:2(OOH), which were formed by oxidation of one of the linoleic acyl chains; little was known previously regarding the presence of this TAG in WAT. The hydrophobic environment in WAT would contribute to the stability, even though the hydroperoxy acyl chain of TAG is considered an unstable structure. In other instances, 18:2–18:2–18:2(OOH) (m/z 928.76), 16:0–18:2–18:2(OOH) (m/z 904.76) and 16:0–16:0–18:2(OOH) (m/z 880.76) TAGs were similarly determined based on individual hydroperoxy DAG and DAG ion products, and hydroperoxy MAG and MAG ion products (Fig. 5B–D). These hydroperoxy TAGs in WAT might be sources of precursors for some oxidized fatty acid mediators during the progress of obesity or succeeding inflammation [19,20].

For example, in our preliminary experiment, increase of hydroperoxy TAGs was observed in some obese model mice at inflamed sites and these TAGs might be available for indication of obesity and succeeding inflammation (manuscript in preparation).

From the presentation of individual TAG structures on the 2D map, the WAT also contained more TAG molecular species containing short-chain SFA and MUFA (Fig. 6 and Table 2) than mouse liver (Fig. 4 and Table 1). These findings demonstrate that the 2D profiles using our method are effective in globally examining different distribution patterns of TAG molecular species and detecting novel molecules such hydroperoxy TAGs, because neutral loss scanning is insufficient to discriminate among the close m/z value TAGs without separating them by LC.

Our method remains to be solved for the quantitative evaluation of TAG molecular species readily from the 2D map, because abundance of individual TAGs was adjusted by the color gradient. But, the difference of TAG profiles is readily detected from the sensitive 2D map using our method and the variations of TAGs including the minor molecular species are easily obtained. For the further global quantitative analysis, we are trying to create three-dimensional maps, constructed with X (retention time), Y (m/z value) and Z (intensity) axes, and to prepare the automated differential display system as subtraction maps.

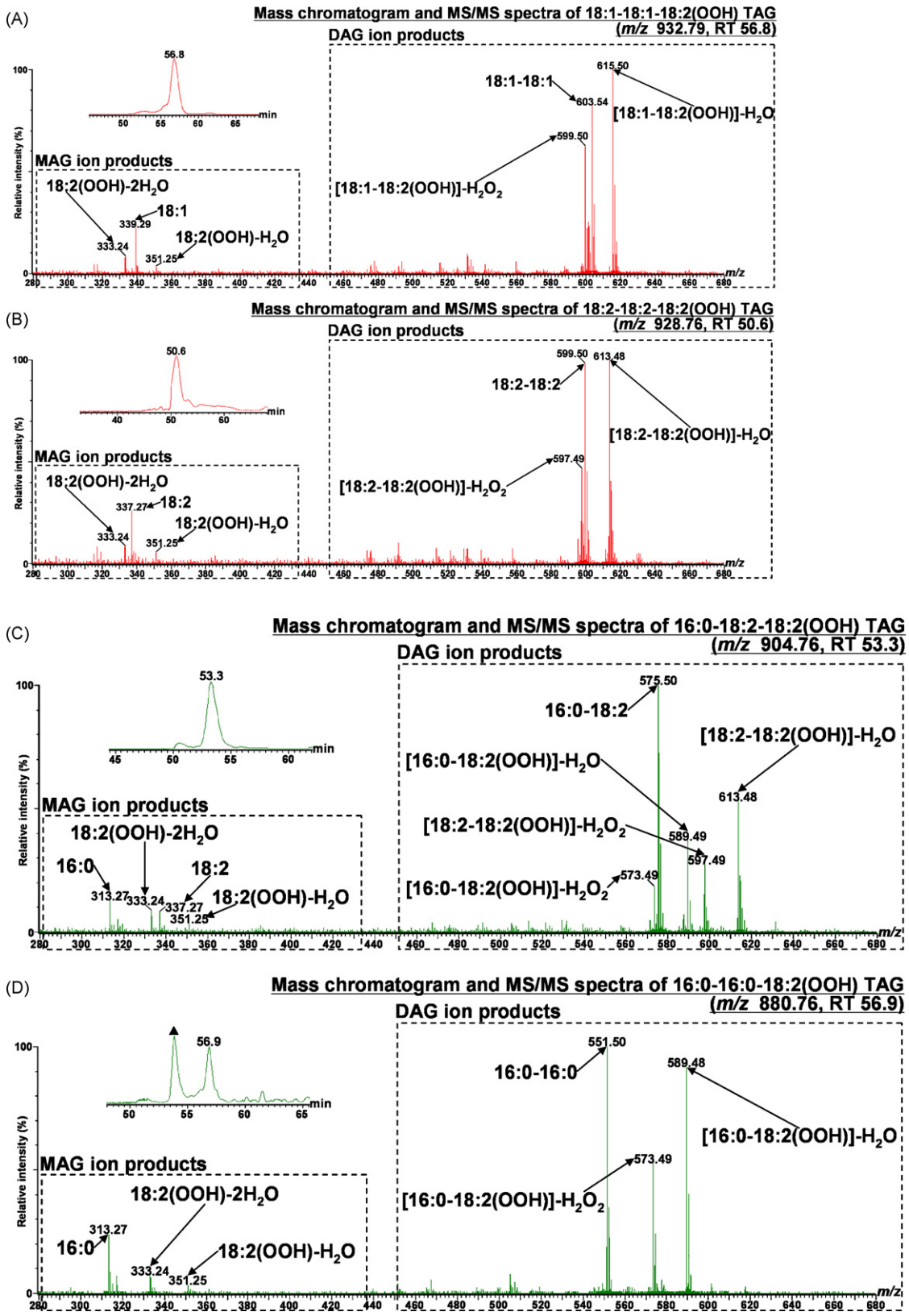

Fig. 5. Mass chromatogram and MS/MS spectra of (A) 18:1–18:1–18:2(OOH) (*m*/*z* 932.79), (B) 18:2–18:2–18:2(OOH) (*m*/*z* 928.76), (C) 16:0–18:2–18:2(OOH) (*m*/*z* 904.76) and (D) 16:0–16:0–18:2(OOH) (*m*/*z* 880.76) TAGs from mouse WAT by reverse-phase high resolution LC/ESI-QTOF MS/MS analysis. Each TAG was determined based on individual hydroperoxy DAG ion products (produced by loss of H_2O or H_2O_2 from [hydroperoxy DAG−OH]$^+$ derived from loss of the fatty acyl residue from the TAG ion) and DAG ion product ([DAG−OH]$^+$ produced by loss of the hydroperoxy linoleic acyl chain from the TAG ion), and on hydroperoxy MAG ion products (produced by loss of H_2O or $2H_2O$ from [hydroperoxy MAG−OH]$^+$ derived from loss of the two fatty acyl residues from the TAG ion) and MAG ion products ([MAG−OH]$^+$ produced by loss of the hydroperoxy acyl chain and fatty acyl residue from the TAG ion). The isotopic peak of other molecular species was indicated by triangle (▲).

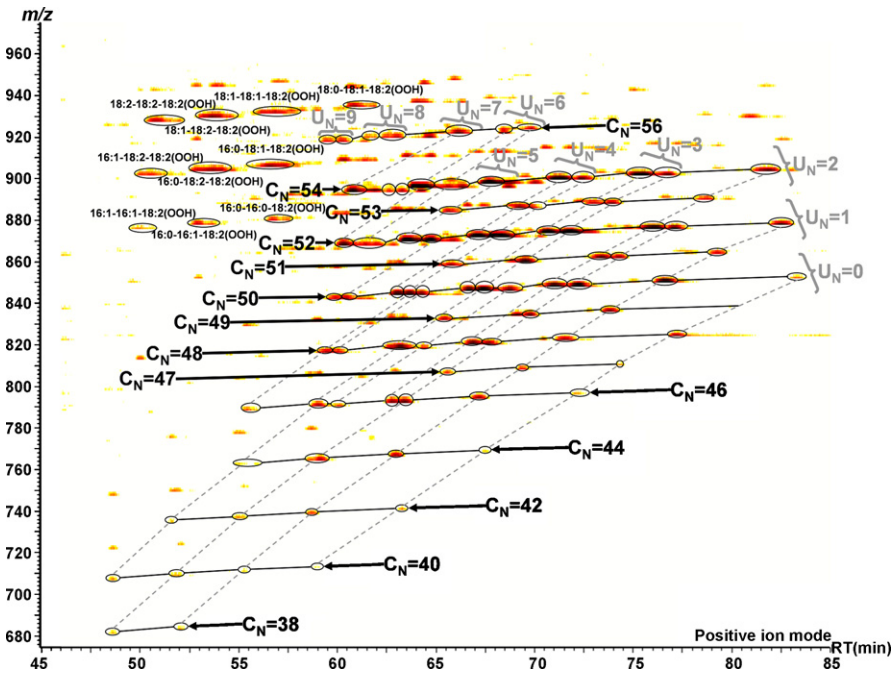

Fig. 6. 2D map of TAG molecular species from mouse WAT by reverse-phase high resolution LC/ESI-QTOF MS/MS analysis. Individual TAG molecular species identified by the MS/MS analysis were present on the 2D map. Many of hydroperoxy TAGs and TAGs containing short-chain saturated fatty acids (SFAs) were characteristically seen in mouse WAT. TAGs with the same total carbon chain length (C_N) and TAGs with the same total degree of unsaturation (U_N) were respectively indicated by solid line and dotted line.

Our method is also capable of analyzing not only TAGs but also PLs, DAGs, SMs and Cers at the same time, so this may be beneficial to elucidate variations of these molecular species more globally for the abnormality of lipid metabolism such as obesity.

4. Conclusion

We have developed a method for global analysis of TAG molecular species including structural isomers, hydroperoxy and odd number acyl carbon chain from the complex lipid mixtures without TAG purification. The 2D profile enables visible and reliable identification of these molecular species and detection of characteristic molecular species such as novel hydroperoxy TAGs in mouse WAT. Our method will be useful for studying changes in the relative profiling of TAG molecular species and identifying lipid biomarkers.

Acknowledgment

This study was performed with the help of Core Research for Evolutional Science and Technology (CREST), Japan Science and Technology Agency (JST).

References

[1] X.D. Rosen, B.M. Spiegelman, Nature 444 (2006) 847.
[2] R.H. Unger, Trends Endocrinol. Metab. 14 (2003) 398.
[3] R.A. Coleman, D.P. Lee, Prog. Lipid Res. 43 (2004) 134.
[4] F. Snyder, N. Stephens, Biochim. Biophys. Acta 34 (1959) 244.
[5] D.M. Schwartz, N.E. Wolins, J. Lipid Res. 48 (2007) 2514.
[6] X. Han, R.W. Gross, Anal. Biochem. 295 (2001) 88.
[7] W.C. Byrdwell, W.E. Neff, Rapid Commun. Mass Spectrom. 16 (2002) 300.
[8] H.R. Mottram, R.P. Evershed, J. Chromatogr. A 926 (2001) 239.
[9] R. Taguchi, M. Nishijima, T. Shimizu, Methods Enzymol. 432 (2007) 185.
[10] T. Houjou, K. Yamatani, M. Imagawa, T. Shimizu, R. Taguchi, Rapid Commun. Mass Spectrom. 19 (2005) 654.
[11] L.D. Roberts, G. McCombie, C.M. Titman, J.L. Griffin, J. Chromatogr. B: Anal. Technol. Biomed. Life Sci. 871 (2008) 174.
[12] R.W. Gross, X. Han, Methods Enzymol. 433 (2007) 90.
[13] J. Krank, R.C. Murphy, R.M. Barkley, E. Duchoslav, A. McAnoy, Methods Enzymol. 432 (2007) 20.
[14] X. Han, R.W. Gross, J. Lipid Res. 44 (2003) 1071.
[15] R.C. Murphy, P.F. James, A.M. McAnoy, J. Krank, E. Duchoslav, R.M. Barkley, Anal. Biochem. 366 (2007) 59.
[16] E.G. Bligh, W.J. Dyer, Can. J. Biochem. Physiol. 37 (1959) 911.
[17] C. Cheng, M.L. Gross, E. Pittenauer, Anal. Chem. 70 (1998) 4417.
[18] F. Giuffrida, F. Destaillats, L.H. Skibsted, F. Dionisi, Chem. Phys. Lipids 131 (2004) 41.
[19] G.S. Hotamisligil, Nature 444 (2006) 860.
[20] C.N. Lumeng, J.L. Bodzin, A.R. Saltiel, J. Clin. Invest. 117 (2007) 175.